Supporting Information

The cysteine residue-bridged dinuclear Ni-Fe complexes related to [NiFe]-H_2ases

Li-Cheng Song,* Zhen-Qing Zhang, Zhen-Chao Gu, and Kai-Yu Jiang

Department of Chemistry, State Key Laboratory of Elemento-Organic Chemistry, College of Chemistry, Nankai University, Tianjin 300071, China

Contents:

1. IR and ^{1}H (^{13}C, ^{31}P) NMR spectra of 1

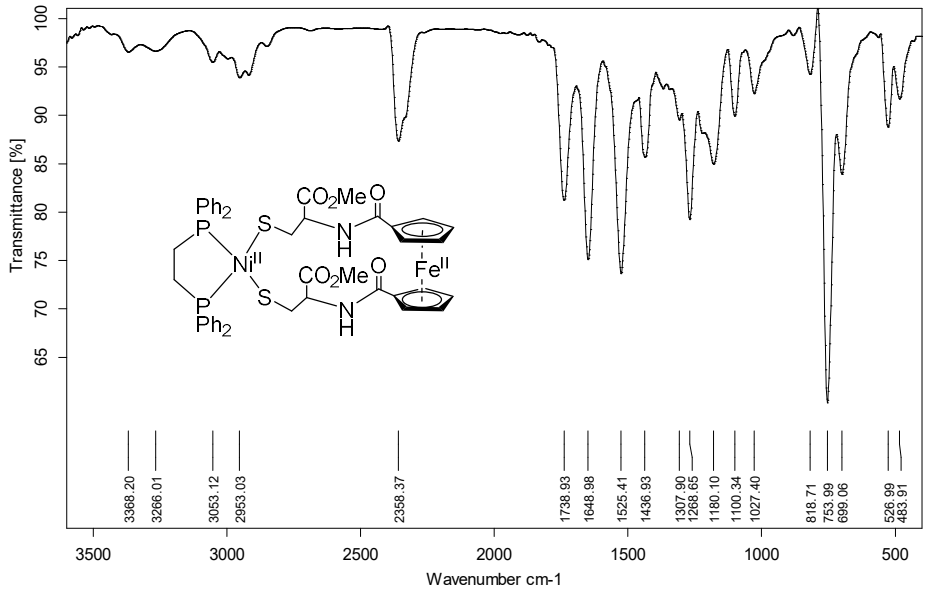

Fig. S1 IR spectrum of **1**

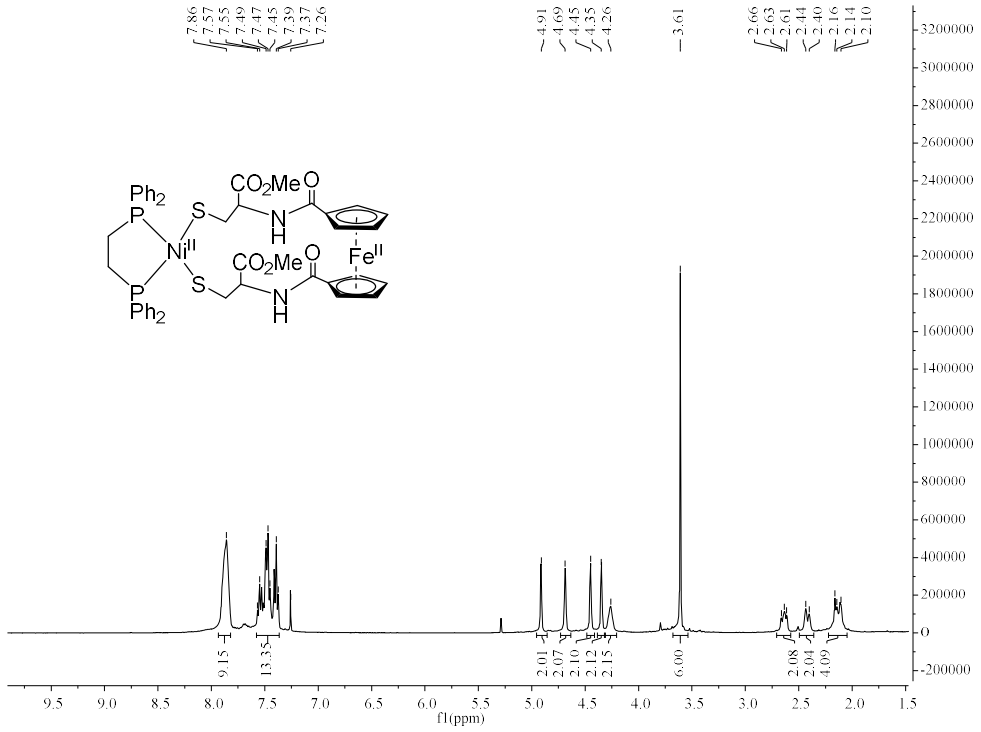

Fig. S2 ^{1}H NMR spectrum of **1**

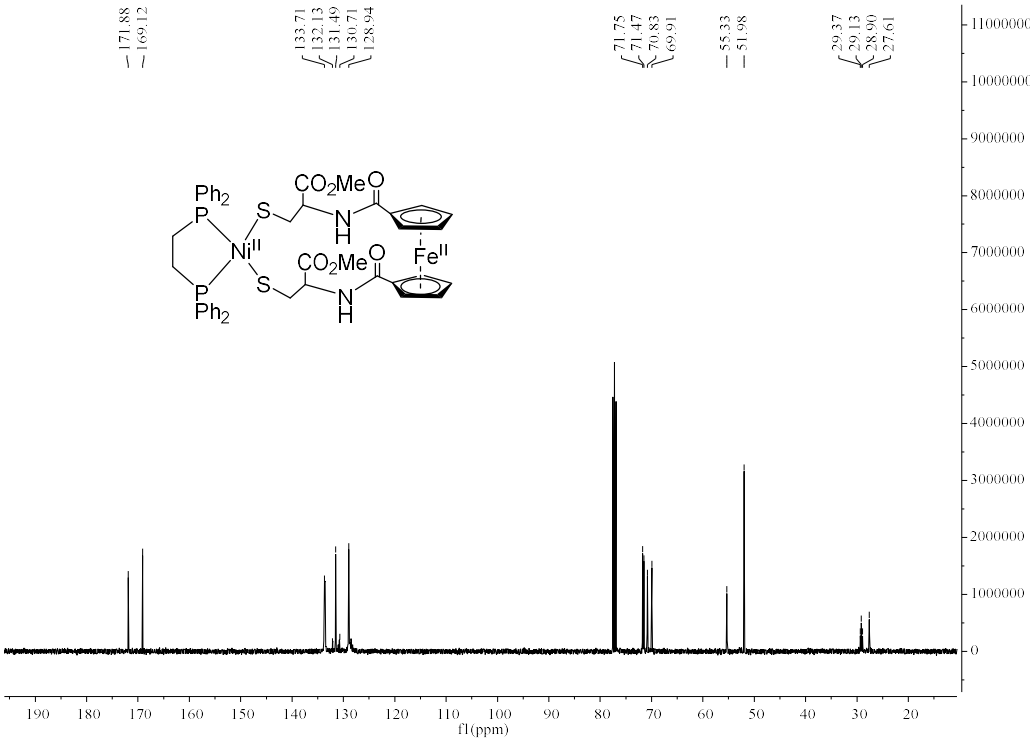

Fig. S3 ^{13}C NMR spectrum of **1**

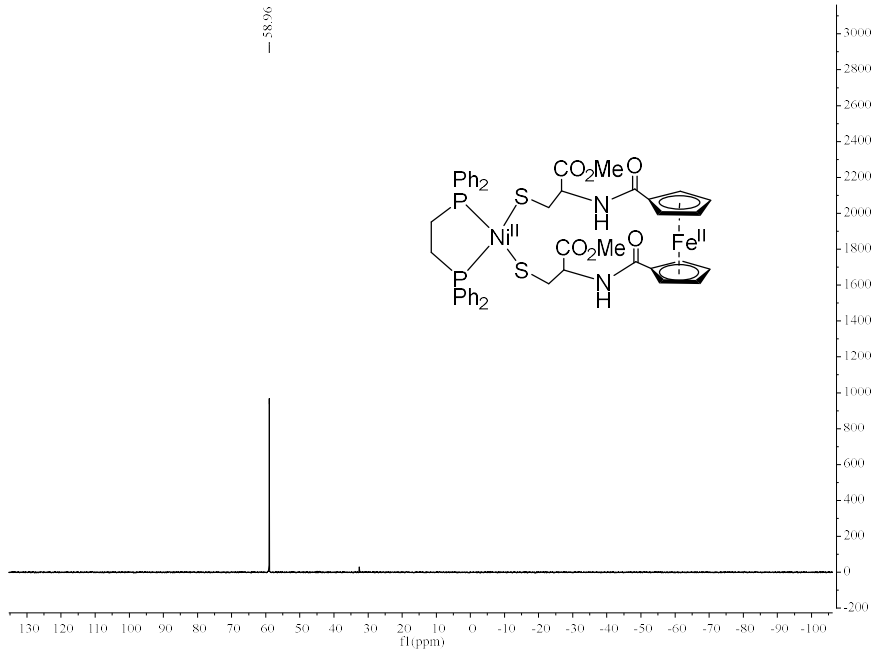

Fig. S4 ^{31}P NMR spectrum of **1**

2. IR and ^{1}H (^{13}C, ^{31}P) NMR spectra of 2

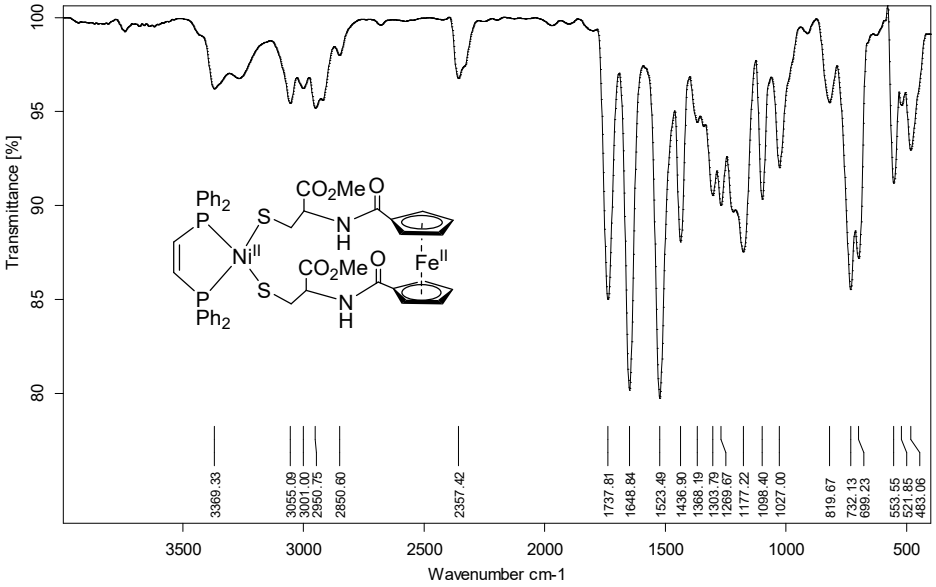

Fig. S5 IR spectrum of **2**

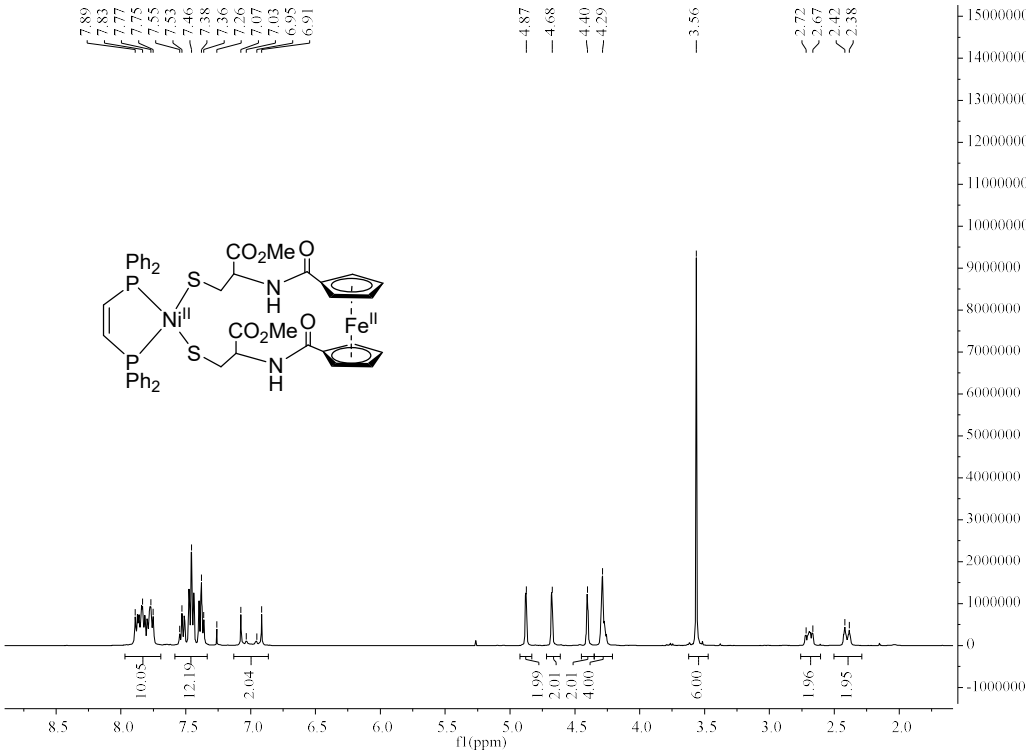

Fig. S6 ^{1}H NMR spectrum of **2**

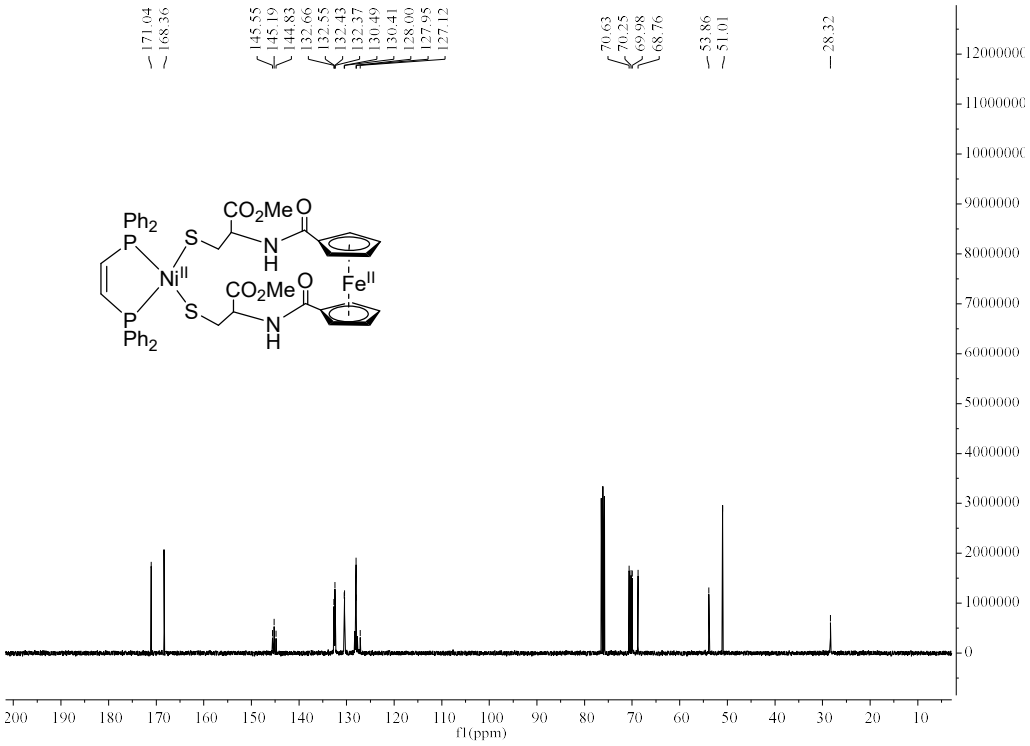

Fig. S7 ^{13}C NMR spectrum of **2**

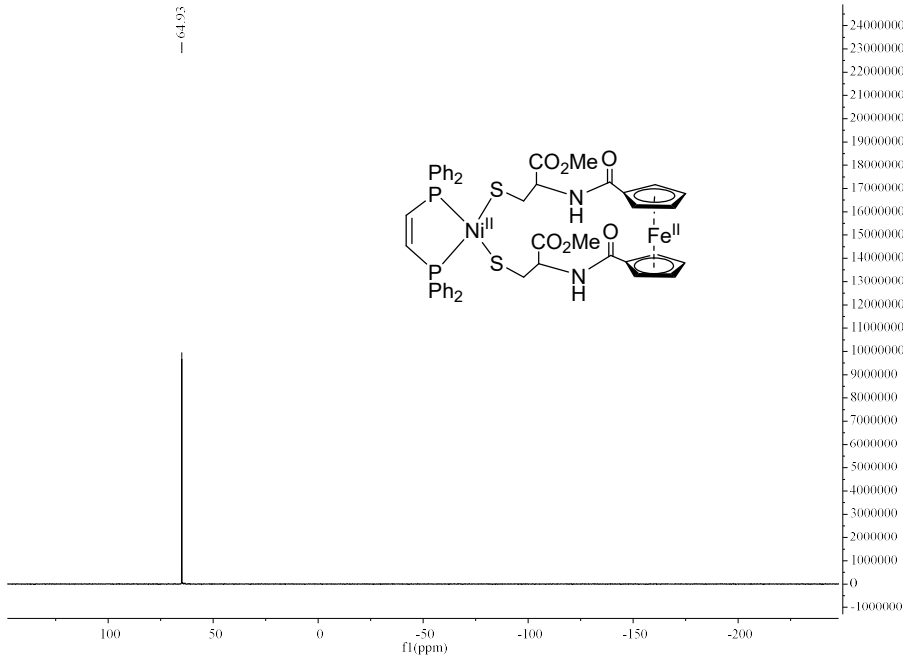

Fig. S8 ^{31}P NMR spectrum of **2**

3. IR and ^{1}H (^{13}C, ^{31}P) NMR spectra of 3

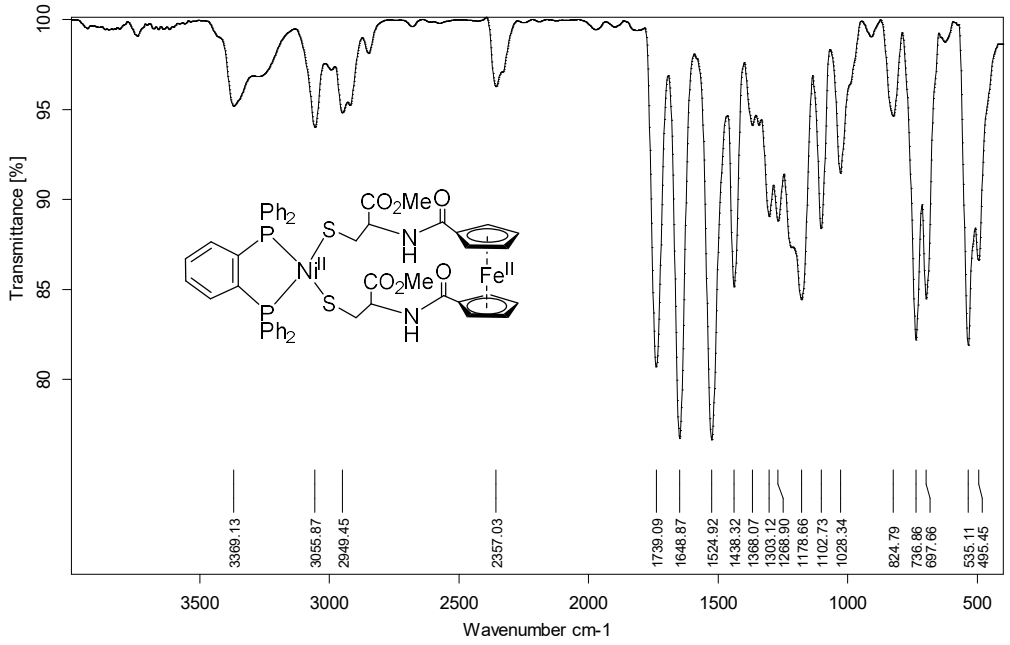

Fig. S9 IR spectrum of **3**

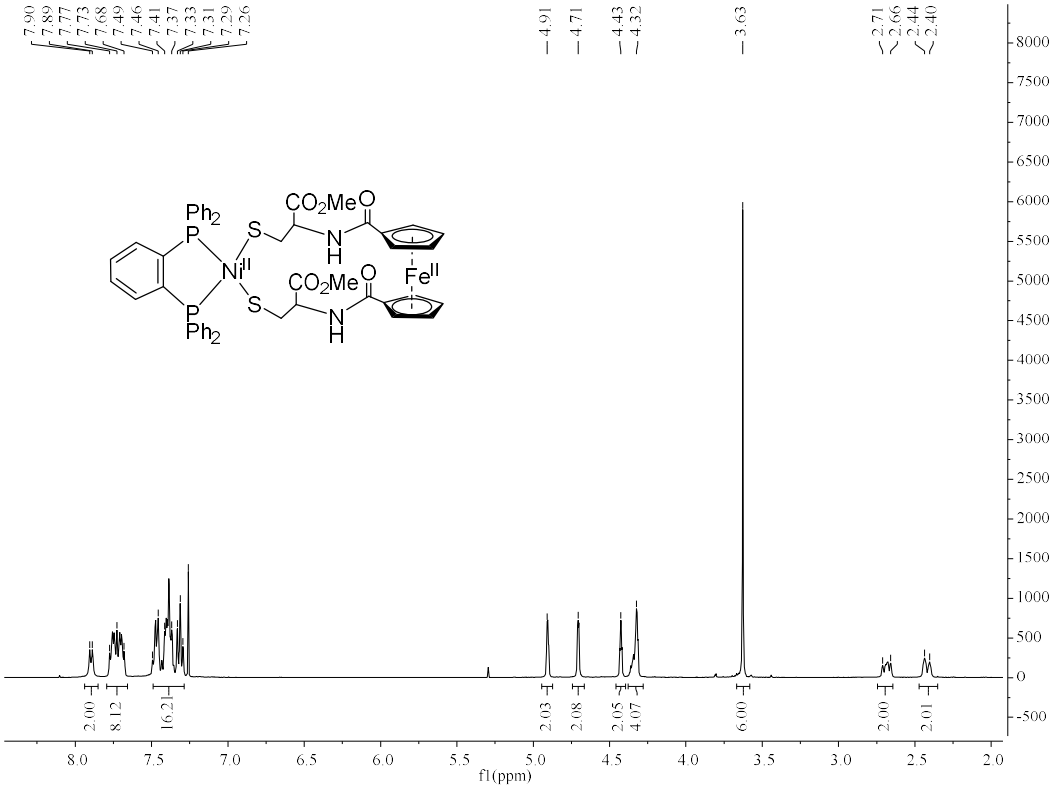

Fig. S10 ^{1}H NMR spectrum of **3**

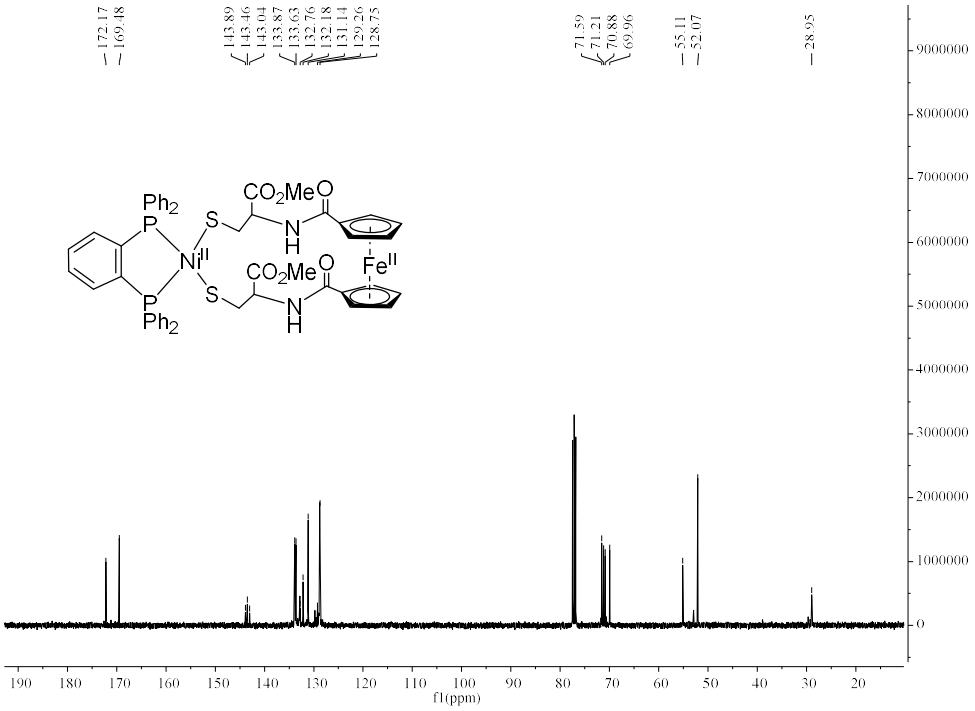

Fig. S11 ^{13}C NMR spectrum of **3**

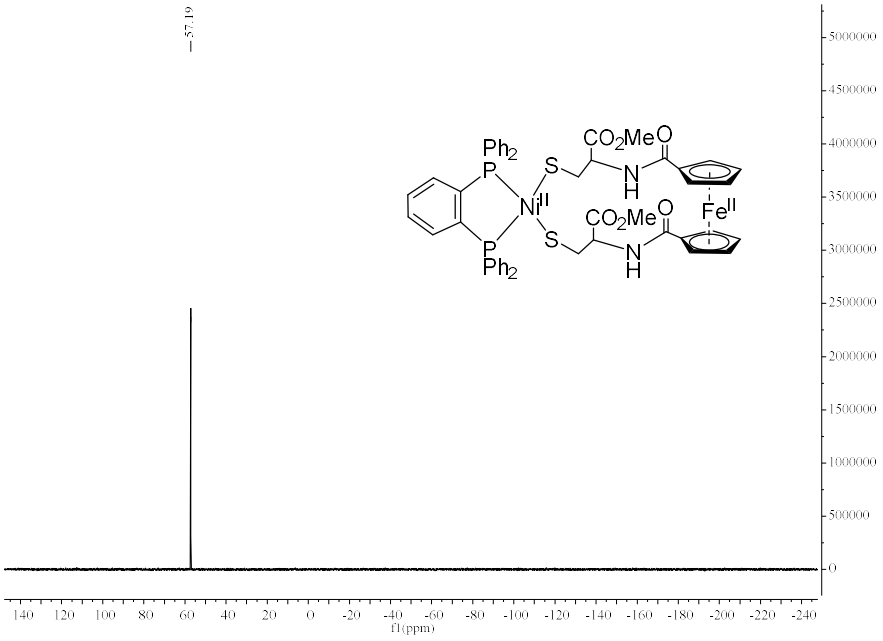

Fig. S12 ^{31}P NMR spectrum of **3**

4. IR and ^{1}H (^{13}C, ^{31}P) NMR spectra of 4

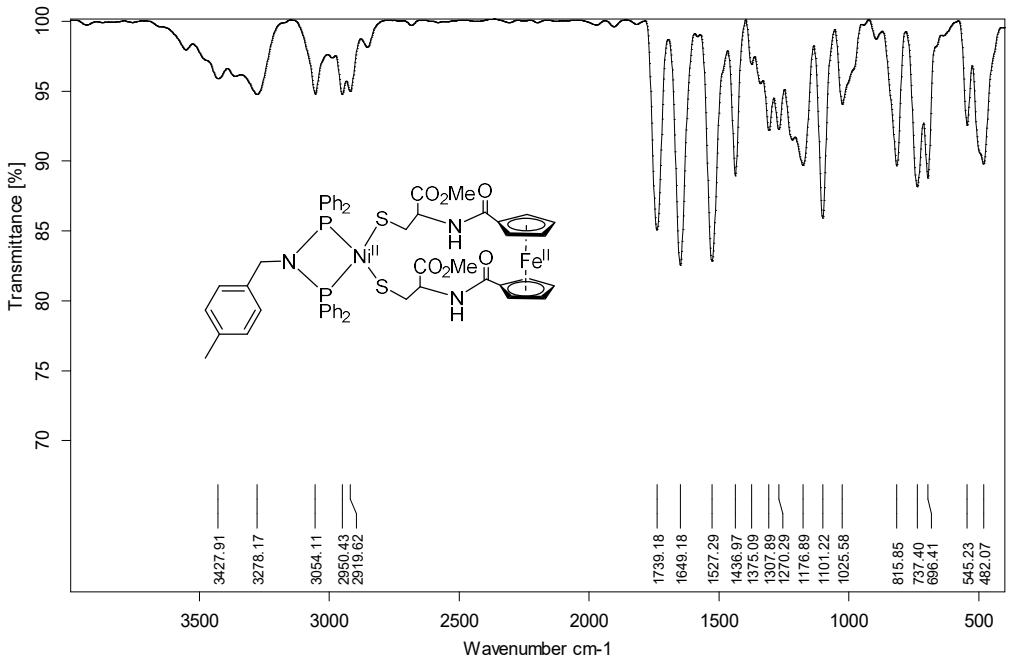

Fig. S13 IR spectrum of **4**

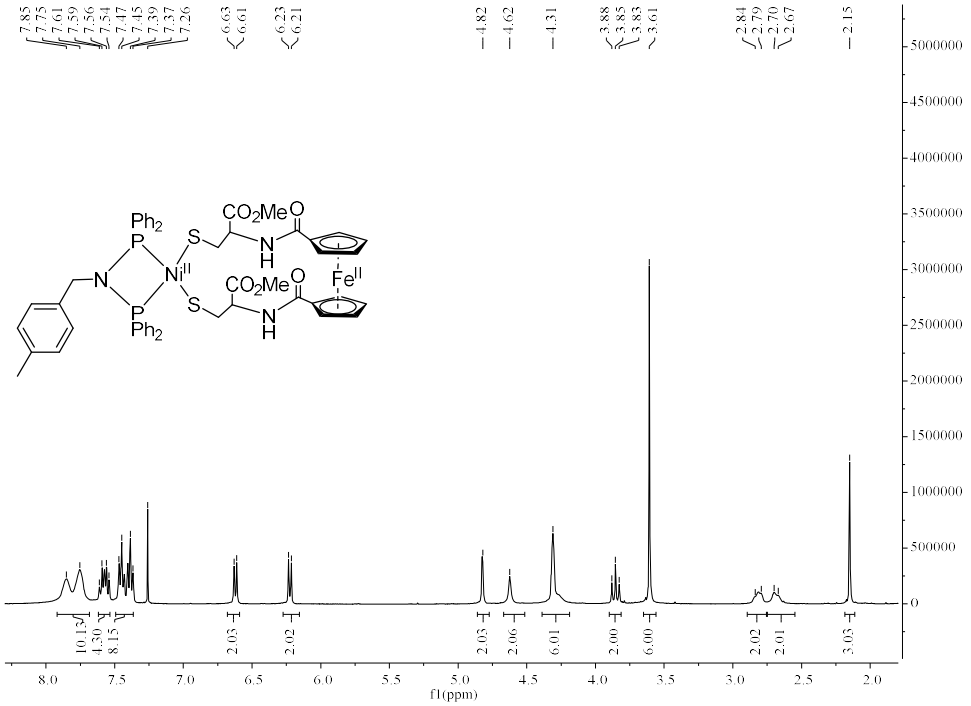

Fig. S14 ^{1}H NMR spectrum of **4**

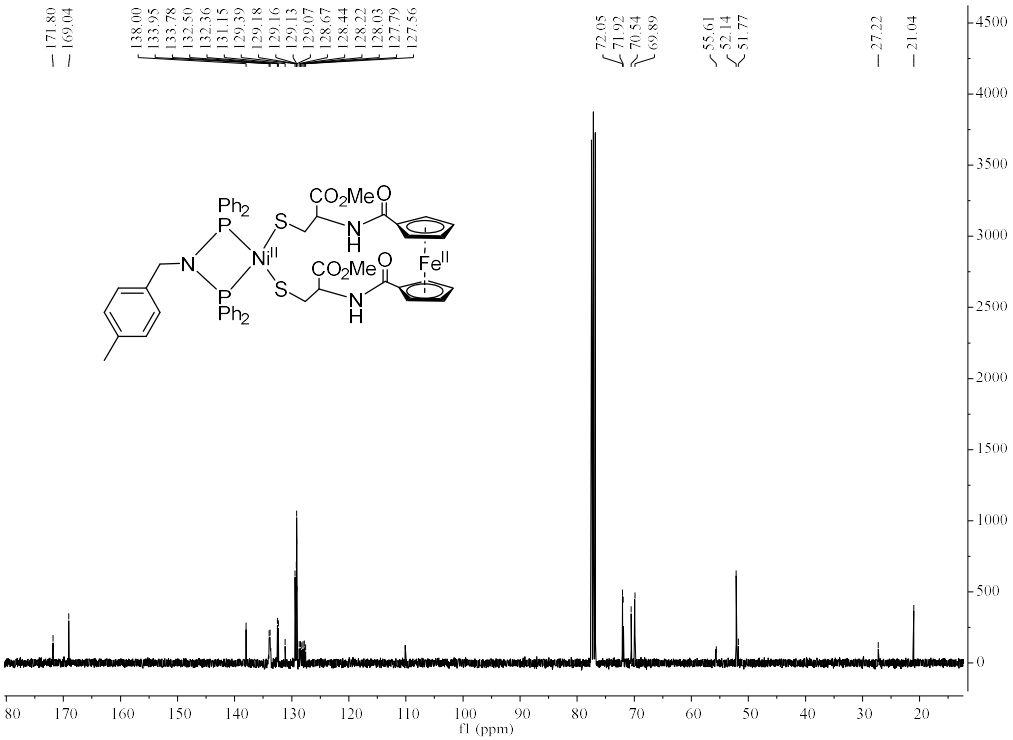

Fig. S15 ^{13}C NMR spectrum of **4**

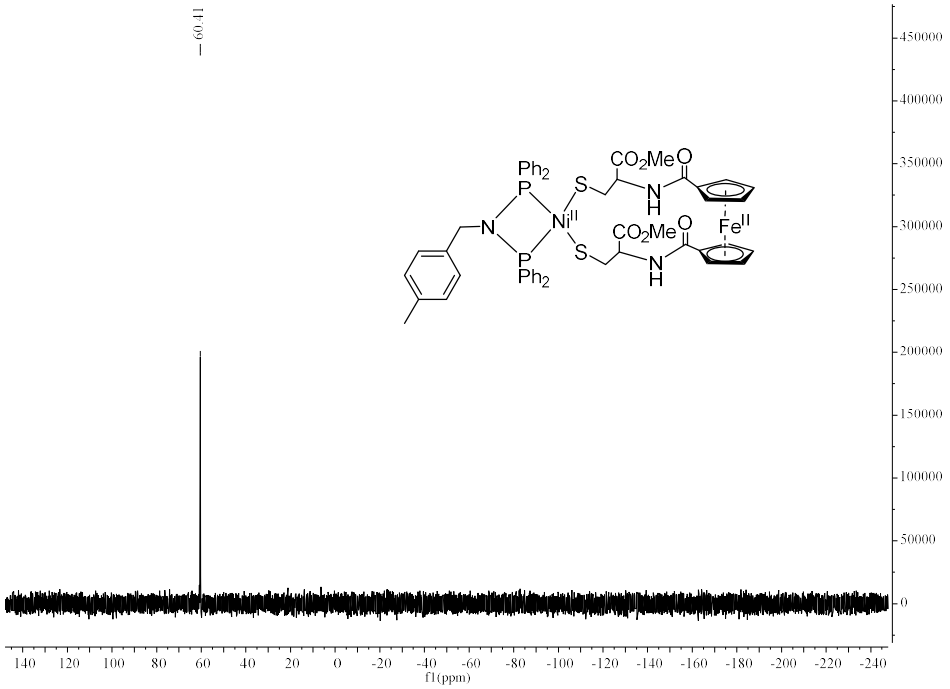

Fig. S16 ^{31}P NMR spectrum of **4**

5. IR and ^{1}H (^{13}C, ^{31}P) NMR spectra of 5

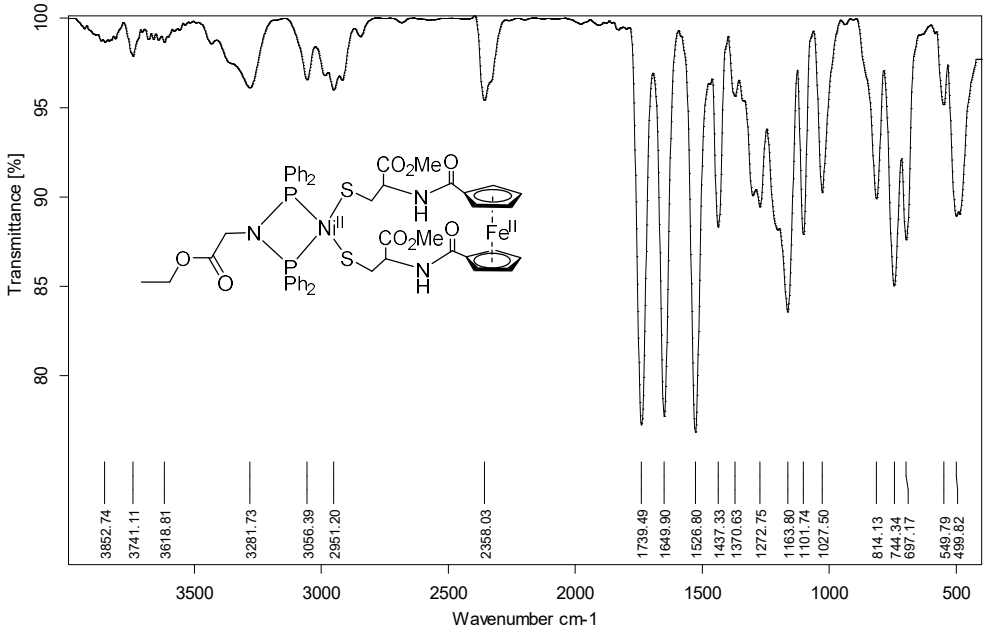

Fig. S17 IR spectrum of **5**

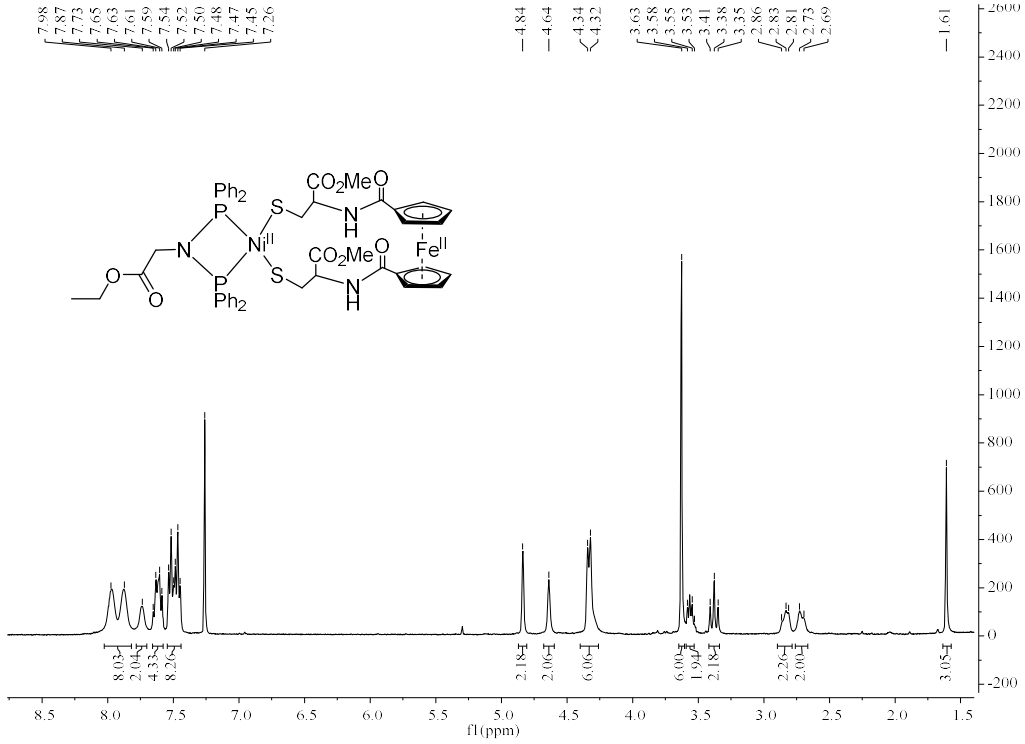

Fig. S18 ^{1}H NMR spectrum of **5**

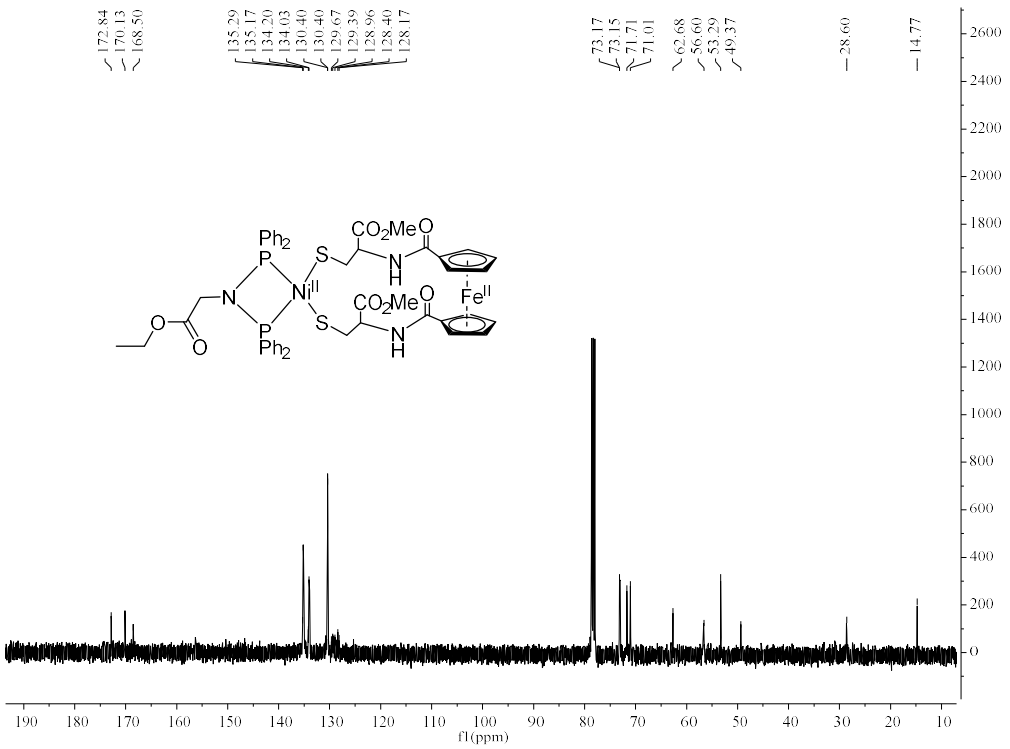

Fig. S19 ^{13}C NMR spectrum of **5**

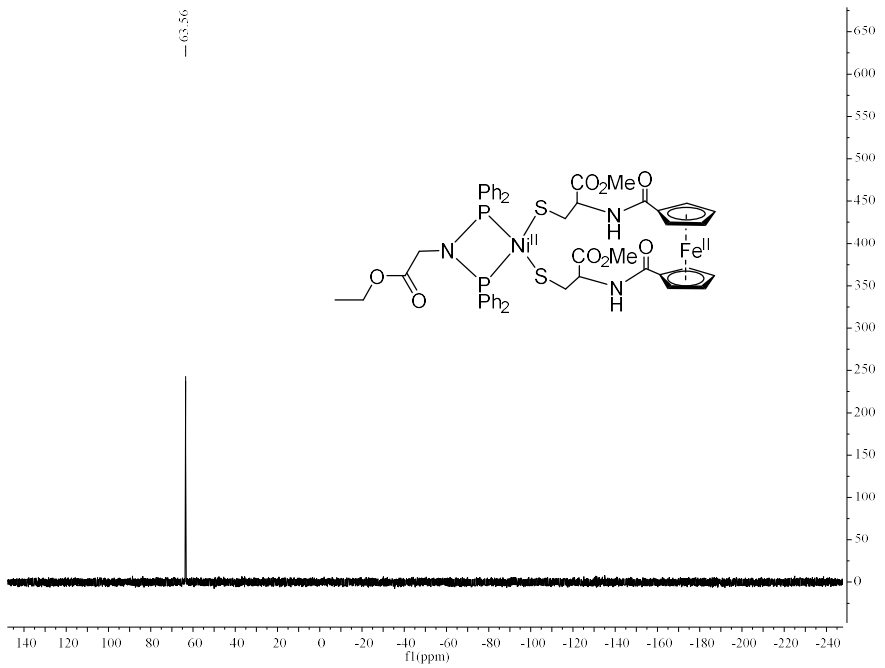

Fig. S20 ^{31}P NMR spectrum of **5**

6. IR and ^{1}H (^{13}C, ^{31}P) NMR spectra of 6

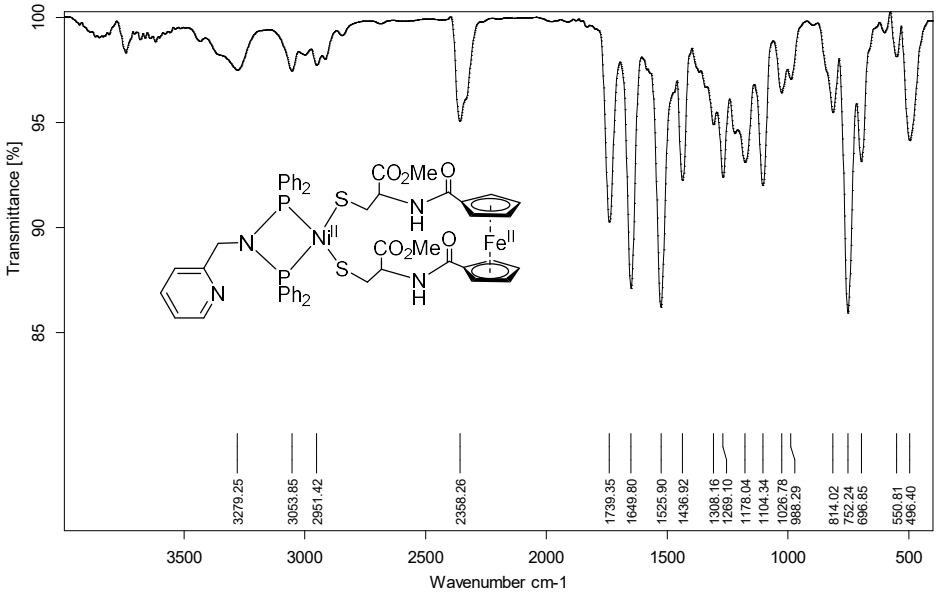

Fig. S21 IR spectrum of **6**

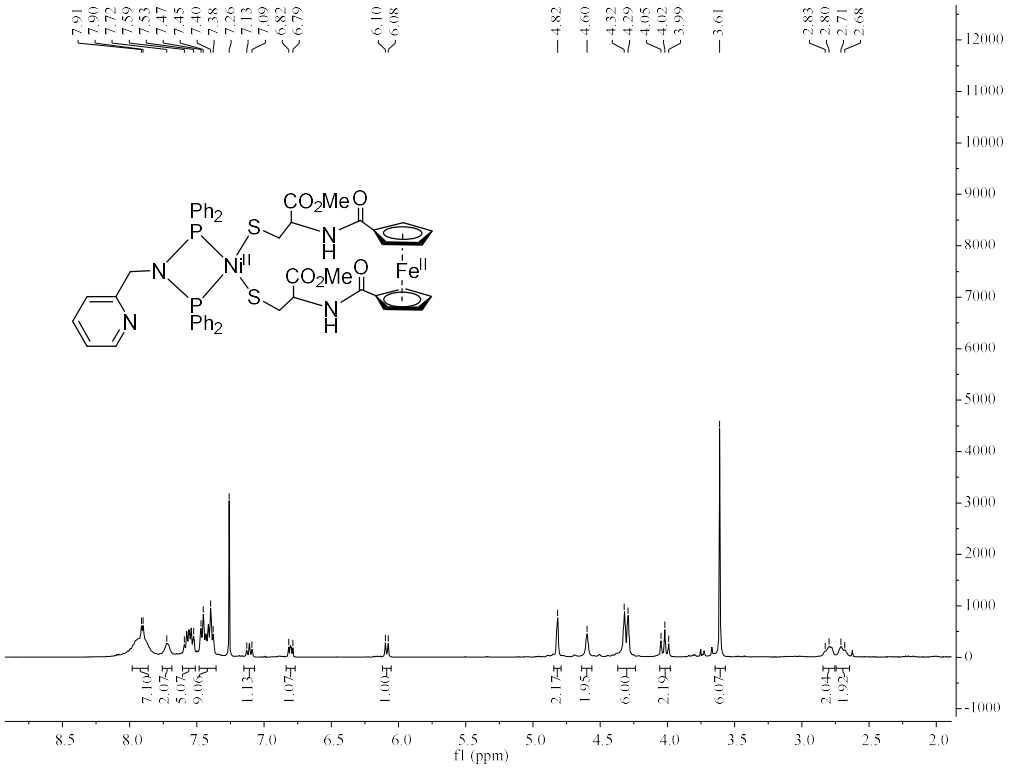

Fig. S22 ^{1}H NMR spectrum of **6**

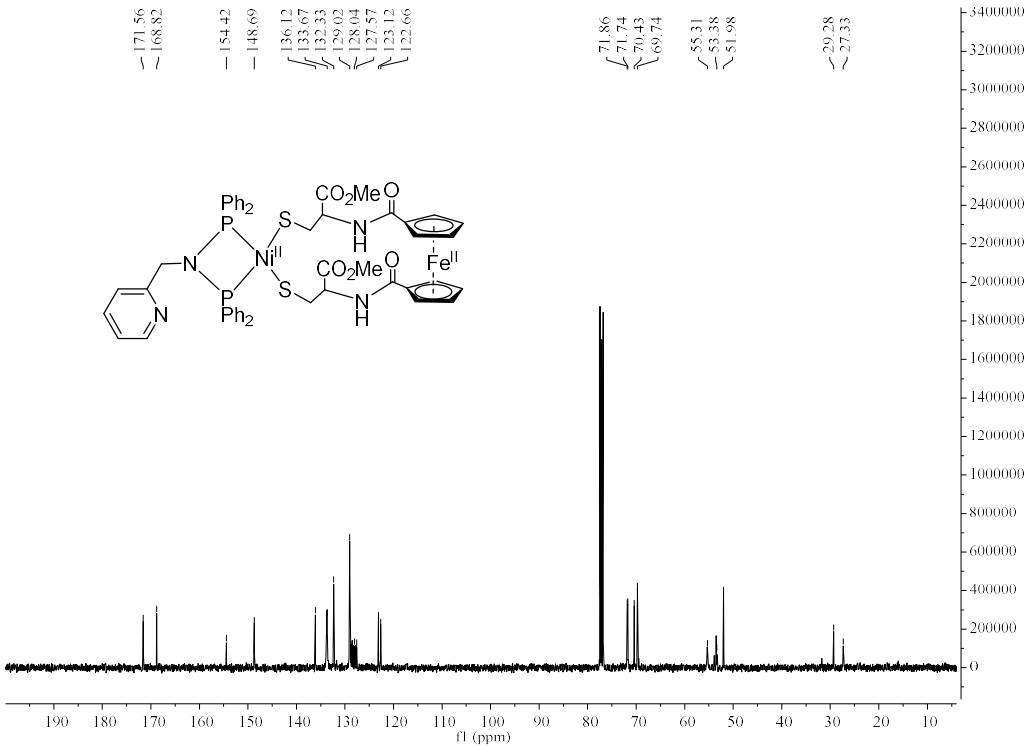

Fig. S23 ^{13}C NMR spectrum of **6**

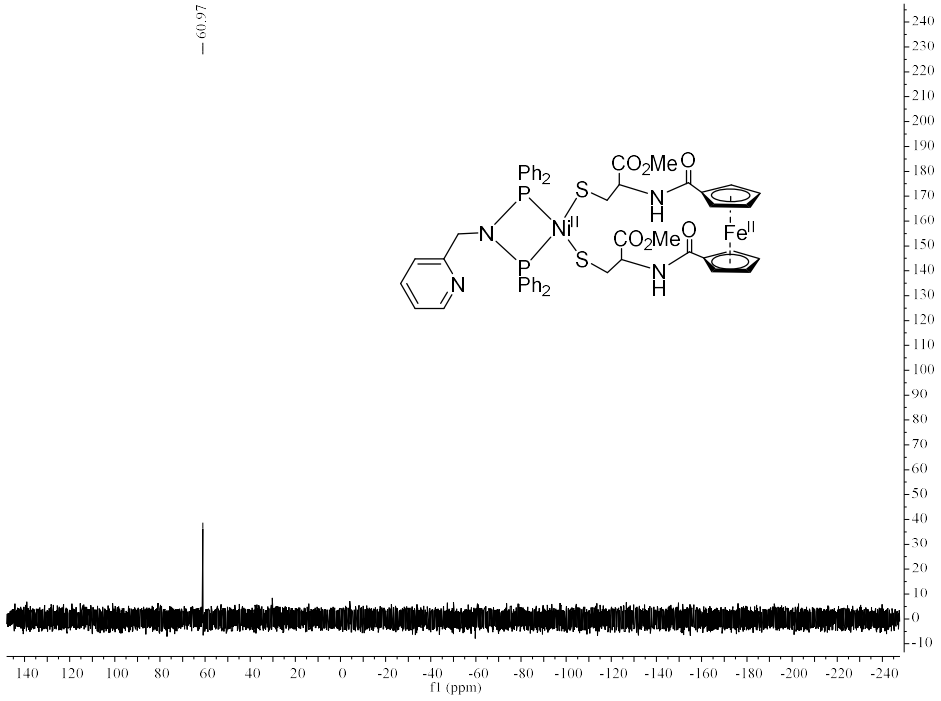

Fig. S24 ^{31}P NMR spectrum of **6**

7. Controlled-potential electrolysis (CPE) for the two-electron reduction of $[CpFe(CO)_2]_2$ and the one-electron reductions for the first reduction events of 1 and 4

The first reduction events for **1** and **4** are one-electron processes since their final Q values determined by CPE are almost close to half that of the known two-electron reduction process of dimer $[CpFe(CO)_2]_2$.[1,2]

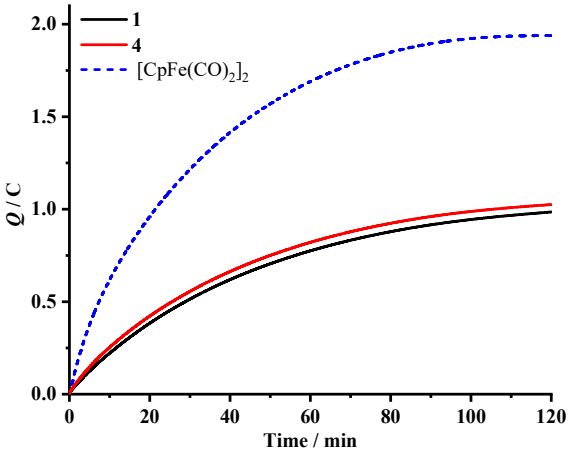

Fig. S25 CPE for the two-electron reduction of $[CpFe(CO)_2]_2$ and the one-electron reductions for the first reduction events of **1** and **4**.

8. Controlled-potential electrolysis (CPE) for the two-electron reduction of $[CpFe(CO)_2]_2$ and the one-electron oxidations for the first oxidation events of 1 and 4

The first oxidation events for **1** and **4** are one-electron processes since their final Q values determined by CPE are almost close to half that of the known two-electron reduction process of dimer $[CpFe(CO)_2]_2$.[1,2]

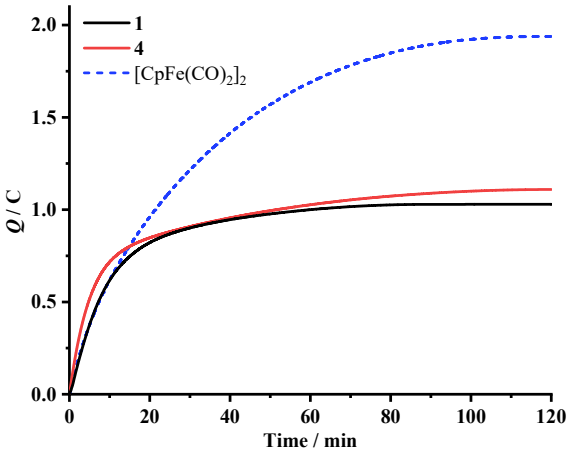

Fig. S26 CPE for the two-electron reduction of $[CpFe(CO)_2]_2$ and the one-electron oxidations for the first oxidation events of **1** and **4**.

9. Cyclic voltammogram of bis(1,1′-ketocysteine)ferrocene

Fe[η^5-$C_5H_4CONHCH(CO_2Me)CH_2SH]_2$（A）

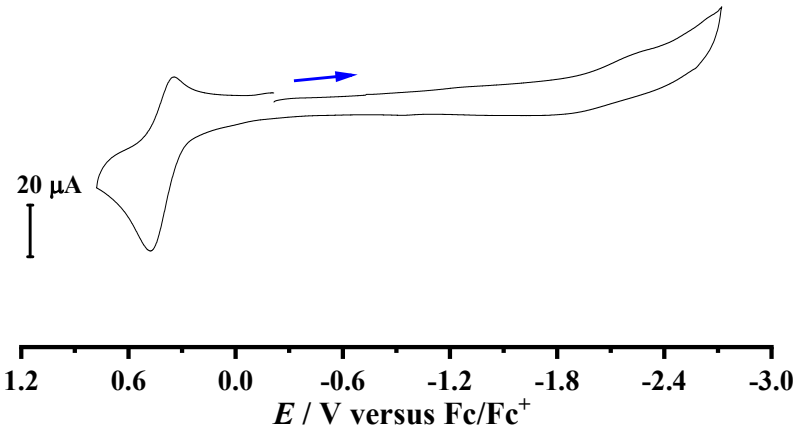

Fig. S27 Cyclic voltammogram of complex **A** (1.0 mM) in 0.1 M *n*-Bu_4PF_6/MeCN at a scan rate of 0.1 V s^{-1}. Arrow indicates the starting potential and scan direction.

10. Cyclic voltammograms in HOAc in the presence of catalyst 1 or 4 and without 1 or 4 in MeCN

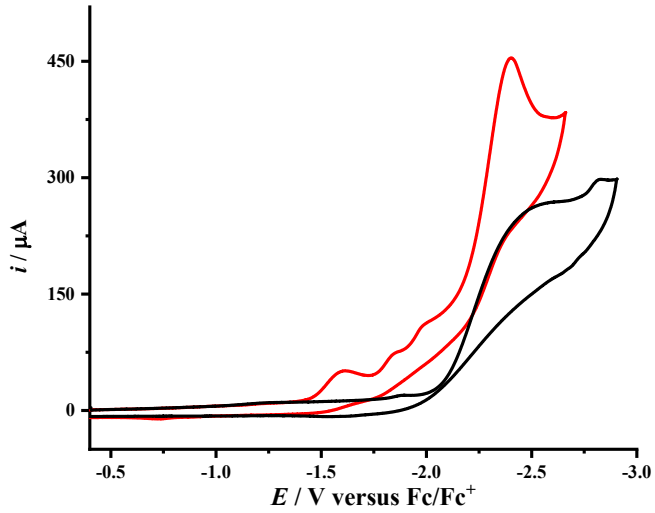

Fig. S28 Cyclic voltammograms in 40 mM HOAc in the presence of 1.0 mM catalyst **1** (red line) and without **1** (black line) in 0.1 M *n*-Bu_4NPF_6 at a scan rate of 0.1 V s^{-1}.

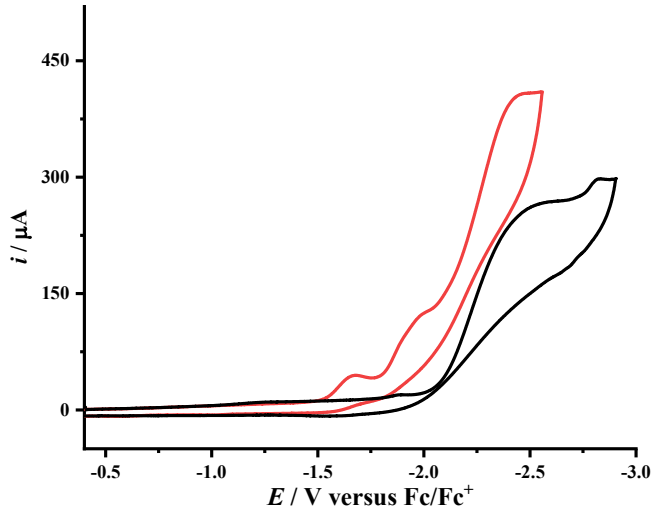

Fig. S29 Cyclic voltammograms in 40 mM HOAc in the presence of 1.0 mM catalyst **4** (red line) and without **4** (black line) in 0.1 M *n*-Bu_4NPF_6 at a scan rate of 0.1 V s^{-1}.

11. Dependence of i_{cat}/i_p for 1 and 4 upon HOAc concentration in MeCN

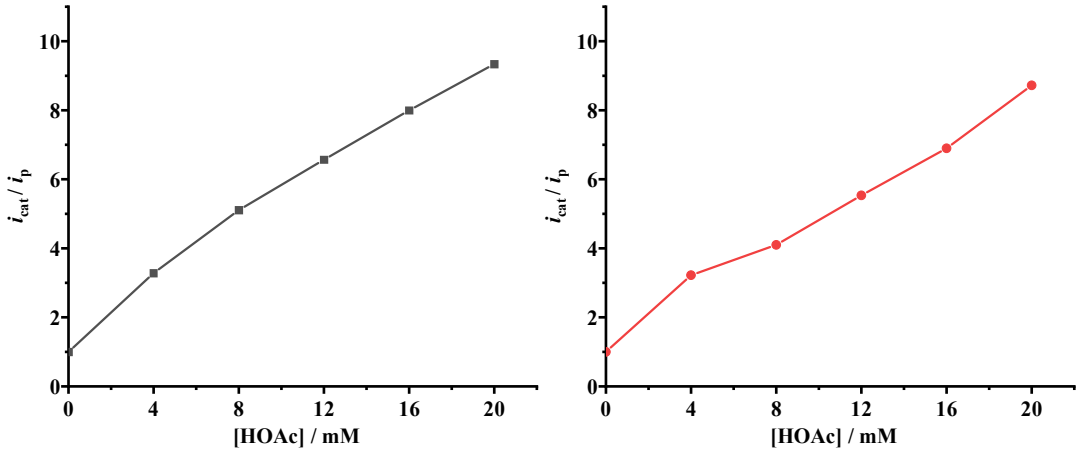

Fig. S30 Dependence of i_{cat}/i_p for complexes **1** (■) and **4** (●) (1.0 mM) upon HOAc concentration (0, 4, 8, 12, 16, 20 mM) in MeCN.

12. Overpotential determinations for 1 and 4 with HOAc in MeCN

Since the pK_a and the standard redox potential of HOAc in MeCN (pK_a^{MeCN} = 22.3, $E^\circ_{H^+/H2}$ = −0.028 V)[3,4] are known, the equilibrium potential (E°_{HA} = −1.35 V vs Fc/Fc$^+$) can be calculated according to eq. S1 using Evans relationship. The overpotentials of the electrocatalytic proton reductions catalyzed by **1** and **4** were measured using eq. S2 from the potential at 0.5 (i_{pc}), where i_{pc} is the cathodic peak current in the cyclic voltammograms recorded after addition of 20 mM of HOAc.

$$E^\circ_{HA} = E^\circ_{H^+/H2} - (2.303RT/F)\, pK_{a,HA} \qquad \text{eq.S1}$$

$$\text{overpotential} = |E^\circ_{HA} - E_{cat/2}| \qquad \text{eq.S2}$$

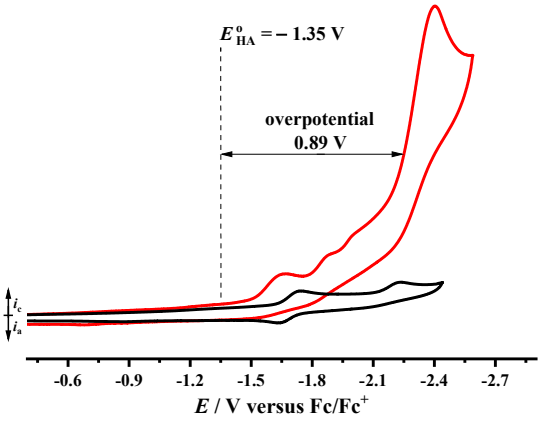

Fig. S31 Cyclic voltammograms of **1** (1.0 mM) with HOAc (0, 20 mM) in 0.1 M *n*-Bu$_4$NPF$_6$/MeCN at a scan rate of 0.1 V s^{-1}.

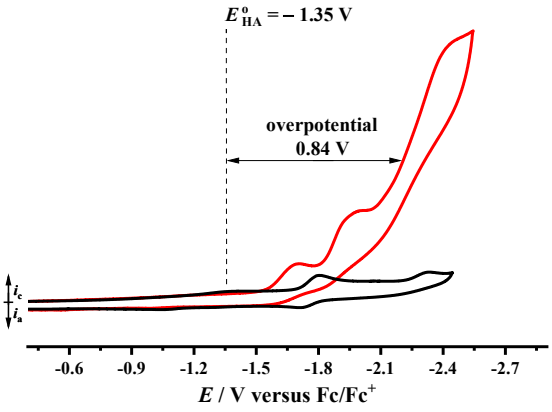

Fig. S32 Cyclic voltammograms of **4** (1.0 mM) with HOAc (0, 20 mM) in 0.1 M *n*-Bu$_4$NPF$_6$/MeCN at a scan rate of 0.1 V s^{-1}.

13. CPE experiments with 50 mM HOAc in MeCN for hydrogen evolution reaction (HER) catalyzed by 1 and 4

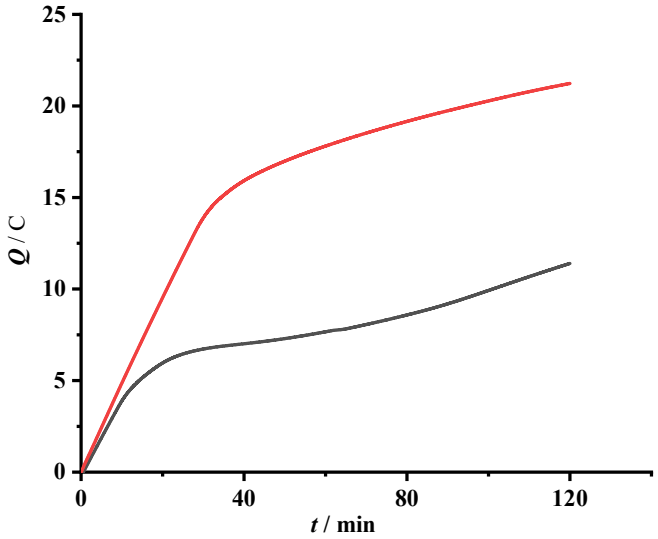

Fig. S33 CPE of **1** (1.0 mM, red line) and blank (no catalyst, black line) with 50 mM HOAc in 0.1 M *n*-Bu_4NPF_6/MeCN at -2.45 V.

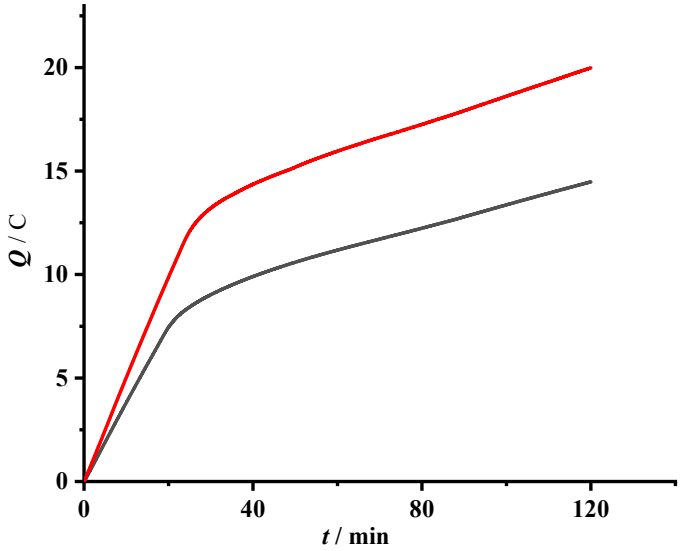

Fig. S34 CPE of **4** (1.0 mM, red line) and blank (no catalyst, black line) with 50 mM HOAc in 0.1 M *n*-Bu_4NPF_6/MeCN at -2.50 V.

References

1 L.-C. Song, X.-F. Han, W. Chen, J.-P. Li and X.-Y. Wang, *Dalton Trans.*, 2017, **46**, 10003-10013.

2 L.-C. Song, Y.-X. Wang, X.-K. Xing, S.-D. Ding, L.-D. Zhang, X.-Y. Wang and H.-T. Zhang, *Chem. Eur. J.*, 2016, **22**, 16304-16314.

3 G. A. N. Felton, R. S. Glass, D. L. Lichtenberger and D. H. Evans, *Inorg. Chem.*, 2006, **45**, 9181-9184.

4 E. S. Rountree, B. D. McCarthy, T. T. Eisenhart and J. L. Dempsey, *Inorg. Chem.*, 2014, **53**, 9983-10002.